Cell. Mol. Life Sci. 65 (2008) 2943 – 2951
1420-682X/08/182943-9
DOI 10.1007/s00018-008-8300-2

Cellular and Molecular Life Sciences

Research Article

The antioxidant function of Bcl-2 preserves cytoskeletal stability of cells with defective respiratory complex I

A. M. Porcelli[a, *], A. Ghelli[a], L. Iommarini[a], E. Mariani[a], M. Hoque[a], C. Zanna[a], G. Gasparre[b] and M. Rugolo[a]

[a] Dipartimento di Biologia Evoluzionistica Sperimentale, Università di Bologna, Via Irnerio 42, Bologna 40122 (Italy), Fax: +39-051-242576, e-mail: annamaria.porcelli@unibo.it
[b] Unità di Genetica Medica, Policlinico Universitario S. Orsola-Malpighi, Università di Bologna, Bologna 40138 (Italy)

Received 28 May 2008; received after revision 8 July 2008; accepted 29 July 2008
Online First 11 August 2008

Abstract. Human thyroid carcinoma XTC.UC1 cells harbor a homoplasmic frameshift mutation in the MT-ND1 subunit of respiratory complex I. When forced to use exclusively oxidative phosphorylation for energy production by inhibiting glycolysis, these cells triggered a caspase-independent cell death pathway, which was associated to a significant imbalance in glutathione homeostasis and a cleavage of the actin cytoskeleton. Overexpression of the anti-apoptotic Bcl-2 protein significantly increased the level of endogenous reduced glutathione, thus preventing its oxidation after the metabolic stress. Furthermore, Bcl-2 completely inhibited actin cleavage and increased cell adhesion, but was unable to improve cellular viability. Similar effects were obtained when XTC.UC1 cells were incubated with exogenous glutathione. We hence propose that Bcl-2 can safeguard cytoskeletal stability through an antioxidant function.

Keywords. Mitochondria, Bcl-2, cytoskeleton, glutathione, complex I.

Introduction

Remodeling of the cytoskeleton is a fundamental process in many eukaryotic cells. The cytoskeleton is composed of interconnected networks of actin, tubulin and intermediate filaments, which extend throughout the entire cytoplasm of a cell. The existence of a signaling pathway between the mitochondria and cytoskeleton has been reported to be potentially dependent on changes in intracellular ATP, calcium and the mitochondrial membrane potential [1]. Owing to this strict relationship, it is likely that intermediate filament remodeling may occur as a consequence of alterations in the functional state of mitochondria, as a cellular adjustment to energetic impairment. Despite the relevance of this connection, only few studies have been reported so far. One such study documented alterations in vimentin organization in osteosarcoma cells after incubation with the complex IV inhibitor sodium azide [2], while another study has shown alterations in the cytoskeleton in myoblast cultures derived from patients with the m.3243A>G mutation in the mitochondria-coded tRNA for leucine, causing reduced oxidative phosphorylation activity [3].

Mitochondria play a crucial role in the regulation of apoptosis. Both the release of apoptogenic factors and the generation of reactive oxygen species (ROS) from these organelles lead to different modes of cell death. Cytochrome c triggers the formation of the apoptosome, followed by subsequent activation of caspase-9

* Corresponding author.

and downstream caspases [4]. Increased ROS production can influence different cellular targets including transcription factors, signaling pathways and the actin cytoskeleton [5]. The major intracellular antioxidant is the tripeptide glutathione (GSH) that maintains protein thiols in a reduced state and scavenges hydrogen peroxide in a reaction catalyzed by glutathione peroxidase. Recently, GSH has been shown to interact with the anti-apoptotic Bcl-2 protein contributing to its antioxidant-like function at the site of mitochondria [6]. It is generally accepted that the role of Bcl-2 on cell survival is associated with its ability to interact with the pro-apoptotic Bcl-2 family members, such as Bax and BH3-only proteins, thereby inhibiting mitochondrial pro-apoptotic functions [7]. Furthermore, Bcl-2 has been shown to influence mitochondrial metabolism [8, 9]. Finally, Bcl-2 has been reported to increase the stability of the cytoskeleton [10], possibly through interaction with tubulin and paxillin [11, 12].

Through combined genetic and biochemical investigations, we have recently characterized the human thyroid carcinoma XTC.UC1 cell line harboring a homoplasmic frameshift mutation in the MT-ND1 gene of complex I. These cells showed a severe energetic failure at the level of respiratory complex I and suffered a marked loss of viability when exposed to a metabolic stress caused by a strong inhibition of the glycolytic pathway [13]. Under these conditions, obtained by depriving cells of glucose and providing them instead with galactose, cells can only produce ATP through mitochondrial oxidative phosphorylation.

In this study we report that the caspase-independent cell death pathway triggered in XTC.UC1 cells by the forced use of oxidative metabolism was associated to a significant imbalance in GSH homeostasis and a cleavage of the actin cytoskeleton. We then investigated whether Bcl-2 overexpression could protect XTC.UC1 cells from death elicited by metabolic stress. Indeed, Bcl-2 increased the endogenous GSH level and preserved actin integrity and cell morphology. These latter effects were also obtained after incubation with exogenous GSH. We hence propose that Bcl-2 can safeguard cellular morphology and adhesion through its antioxidant function.

Materials and methods

Materials. Sulforhodamine B, ATP monitoring kit, staurosporine, protein A-Sepharose, anti-β-tubulin, protease inhibitors cocktail and glutathione were purchased from Sigma (Milan, Italy). Lipofectamine 2000 was from Invitrogen (Milan, Italy). 7-Amino-4-methylcoumarin, *N*-acetyl-L-aspartyl-L-glutamyl-L-valyl-L-aspartic acid amide (Ac-DEVD-AMC), benzyloxycarbonyl-Val-Ala-Asp-fluoromethyl-ketone (z-VAD-fmk) and Hoechst-33342 were from Calbiochem (La Jolla, CA, USA). Calcein-AM was purchased from Molecular Probes (Invitrogen). Anti-caspase-3 was from Cayman (Ann Arbor, MI, USA), anti-actin and anti-AIF were from Santa Cruz Biotechnology (Santa Cruz, CA, USA), anti-Bcl-2 was from Upstate (Temecula, CA, USA), anti-cytochrome c was from BD Biosciences PharMingen (Milan, Italy) and secondary antibodies were from Jackson ImmunoResearch Europe Ltd (Soham, Cambridgeshire, UK). Anti-HtrA2/Omi was a kind gift from Prof. P. Vandenabeele, Ghent University, Belgium.

Cells and growth conditions. Human thyroid carcinoma XTC.UC1 cells [14] were grown in Dulbecco's modified Eagle's medium (DMEM) containing 10 % fetal bovine serum, 2 mM L-glutamine, 100 U/ml penicillin and 100 µg/ml streptomycin, in a humidified incubator at 37°C with 5 % CO_2. Metabolic stress was induced by incubation in glucose-free DMEM supplemented with 5 mM galactose and 5 mM pyruvate (DMEM-galactose).

Cellular, nuclear, and mitochondrial morphology. Cells (3×10^5) were seeded in 36-mm-diameter dishes and the day after were incubated in DMEM or DMEM-galactose for 24 h. Cellular morphology was observed by optical phase-contrast microscopy with a 40× objective. Nuclear morphology was assessed in cells stained for 30 min with 1 µg/ml Hoechst (excitation at 400 nm and emission at 470 nm). Mitochondrial network was visualized by immunofluorescence analysis using antibody against cytochrome c (1:200), as previously described [15]. The dishes were transferred to the stage of a digital imaging system, comprising an inverted epifluorescence microscope (Diaphot, Nikon, Japan) and Omega Filter pinkel Set XF66–1 triband (Omega Optical Inc., Brattleboro, VT, USA). Images were captured with a back-illuminated Photometrics Cascade CCD camera system (Roper Scientific, Tucson, AZ, USA) and acquisition/analysis software Metamorph (Universal Imaging Corp., Downingtown, PA, USA). Nuclear and mitochondrial morphology was visualized using a 60× 1.4 oil immersion objective.

Total lysates and cytosolic fractions isolation. To obtain total cellular lysates, cells (4×10^6) were resuspended in 0.1 ml RIPA buffer (50 mM Tris-HCl pH 7.6, 150 mM NaCl, 1 % NP-40, 1 % NaDOC, 0.1 % SDS, 5 mM EDTA, 100 µl/ml protease inhibitors cocktail), sonicated and centrifuged at 10 000 *g*.

To isolate the cytosolic fractions, cells were harvested from five 10-cm-diameter dishes, resuspended in 0.5 ml 200 mM mannitol, 70 mM sucrose, 1 mM EGTA, 10 mM HEPES (pH 7.6), 100 µl/ml protease inhibitors cocktail, and homogenized for 40 strokes with a Dounce homogenizer at 4°C. Samples were centrifuged for 10 min at 500 *g*, the resulting supernatants were centrifuged for 10 min at 10 000 *g* and supernatants (cytosolic fractions) were stored at –80 C. Protein content of cell lysates and cytosolic fractions was determined using the Bradford protein assay method, with BSA as a standard [16].

Western blotting. Proteins from total lysates (50 µg) and cytosolic fractions (80 µg) were separated by 12 % SDS-PAGE and transferred onto a nitrocellulose membrane (Bio-Rad, Hertfordshire, UK). The nitrocellulose membranes were incubated with anti-AIF (1:1000), anti-HtrA2/Omi (1:4000), anti-procaspase-3 (1:1000), anti-α-actin (1:500), anti-β-tubulin (1:500), and anti-Bcl2 (1:1000) antibody for 1 h at room temperature. Primary antibodies were visualized using horseradish peroxidase-conjugated secondary antibodies (1:2000). The chemiluminescence signals were revealed using an ECL Western blotting kit (Amersham Bioscience, Buckinghamshire, UK) and measured with the Fluo-2 MAX Multimager system (Bio-Rad).

Caspase-3 activation. Activated caspase-3 can cleave the synthetic substrate Ac-DEVD-AMC; therefore, DEVDase activity was determined in cell lysates (100 µg) by fluorescence measurements as previously described [15]. Caspase-3 activation was also determined by Western blotting (see above).

Measurement of GSH and GSSG. Cells (6×10^6) were grown in 10-cm-diameter dishes and incubated with DMEM or DMEM-galactose. The GSH and glutathione disulfide (GSSG) content was measured enzymatically, as previously described [17]. Briefly, the assay is based on determination of the chromophoric product 2-nitro-5-thiobenzoic acid, resulting from the reaction of 5,5'-dithiobis-(2-nitrobenzoic acid) with GSH. In this reaction, GSH is oxidized to GSSG, which is then reconverted into GSH in the presence of glutathione reductase and NADPH. The rate of 2-nitro-5-thiobenzoic acid formation was measured spectrophotometrically at 412 nm. For GSSG measurement, GSH was derivatized with 2-vinylpyridine and the samples were assayed by mean of the procedure described above for GSH measurement.

Bcl-2 transfection and clone generation. Cells were transfected with the pcDNA3 plasmid containing the full-length *bcl-2* cDNA gene (a gift from G. Manfredi, Weill Medical College of Cornell University, New York, USA) and a pcDNA3 empty vector. Transfection was performed using Lipofectamine 2000 as described by the manufacturer. After 48 h of transfection, clones were selected in the presence of 800 µg/ml G418. Resistant cells were pooled and maintained in culture with 200 µg/ml G418. Clones are indicated as Bcl-2 and mock-transfected cells.

Cell viability and adhesion measurements. After seeding, cells were incubated for 24 h in DMEM or DMEM-galactose. Cell viability was assessed using the colorimetric sulforhodamine B assay [18] and by measuring the cellular ATP content [15]. Quantification of adherent cells was carried out by cell loading with 1 µM calcein-AM (excitation at 488 nm, emission at 520 nm) for 30 min in DMEM or DMEM-galactose. Nonadherent cells were removed by washing, and the number of adherent cells was determined by measuring the fluorescence of the residual cells, quantified at 490 nm using a multilabel counter Wallac 1420 (PerkinElmer Life and Analytical Sciences, Turku, Finland).

Immunoprecipitation. Cell lysates (300 µg) were resuspended in RIPA buffer and mixed with anti-actin (1:200), with anti-β tubulin (1:200) antibodies or with pre-immune serum at 4°C for 2 h. The protein A-Sepharose was added overnight. Precipitates were used for Western blot analysis as described above.

Statistical analysis. All the experiments were repeated at least three times. Results are presented as means ± SD. Statistical analysis was performed using the Student's *t*-test (with $p<0.05$ as the level of significance).

Results

Cell death induced by glycolysis inhibition is associated with actin cleavage. It is widely accepted that incubation of cells in a medium where glucose is replaced by galactose strongly inhibits the rate of the glycolytic pathway and causes a dramatic loss of viability in cells with defective oxidative phosphorylation [19]. As illustrated in Figure 1A, XTC.UC1 cells appeared to shrink significantly and started detaching from the plates after 24-h incubation in DMEM-galactose (Fig. 1A, a and b), being completely detached after 48–72 h, in agreement with our previous report [13]. Analysis of nuclear morphology using the DNA-specific fluorescent dye Hoechst, showed chromatin condensation in cells incubated in

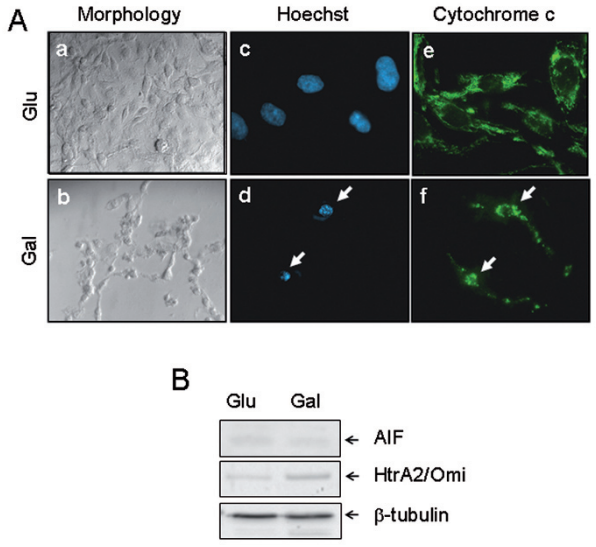

Figure 1. Effect of incubation of XTC.UC1 cells in glucose-free Dulbecco's modified Eagle's medium (DMEM)-galactose. (*A*) Cellular (a, b), nuclear (c, d) and mitochondrial (e, f) morphology were determined after 24-h incubation in DMEM (Glu, a, c, e) or DMEM-galactose (Gal, b, d, f), as described in the Materials and methods. Representative images out of five similar images are shown. The arrows in (d) indicate the same two apoptotic cells analyzed in (f). (*B*) AIF and HtrA2/Omi levels in cytosolic fractions isolated from cells incubated in DMEM (Glu) or DMEM-galactose (Gal). Cytosolic fractions (80 μg) were separated by SDS-PAGE and Western blotting was performed with specific antibodies, as described in Materials and methods. β-Tubulin was used as a control for protein loading. One representative blot out of three blots is shown.

DMEM-galactose (indicated by the arrows in Fig. 1A, d), suggesting an apoptotic type of cell death. To evaluate the mitochondrial network morphology and integrity of XTC.UC1 cells, an immunofluorescence analysis of cytochrome c was performed. In fact, cytochrome c, normally retained within mitochondria, can be released from the organelles during apoptotic cell death and this can be easily evidenced by its diffusion into the cytosol. After 24 h of metabolic stress, the two cells with condensed nuclei (indicated by arrows in Fig. 1A, d) exhibited a fragmented mitochondrial network; however, no cytosolic diffusion of cytochrome c was apparent (Fig. 1A, f). The levels of other apoptogenic proteins such as apoptosis inducing factor (AIF) and HtrA2/Omi were also measured in the cytosolic fractions isolated from XTC.UC1 cells incubated in DMEM or DMEM-galactose by Western blot analysis (Fig. 1B). Quantitative analysis of bands density using β-tubulin as a control for protein loading did not reveal any significant difference between the two conditions, further suggesting that the mitochondria were not involved in the induction of this type of cell death.

To verify this hypothesis, we assessed whether caspases were activated, by determining the cleavage of the fluorogenic caspase-3 and -7 substrate Ac-DEVD-AMC. No DEVDase activity was measured during incubation of cells with DMEM-galactose, whereas an approximately fivefold increase was determined after treatment with 1 μM staurosporine, a positive control (Fig. 2A). Caspase-3 activation was also measured by determining its cleavage by Western blot analysis. The intensity of the protein band of 32 kDa, corresponding to procaspase-3, was not affected during metabolic stress (Fig. 2B). Furthermore, pretreatment of cells with the broad caspase inhibitor z-VAD-fmk (5 μM) failed to significantly increase the viability of cells incubated in DMEM-galactose (Fig. 2C).

In the same samples, the intensity of bands corresponding to the actin cytoskeleton was also measured. After 24-h incubation in DMEM-galactose, the band of 43 kDa corresponding to actin exhibited a time-dependent decrease, associated with the appearance of a new band of approximately 32 kDa (Fig. 2D).

Using dichlorodihydrofluorescein fluorescence, we have previously reported that under basal conditions XTC.UC1 cells produced a significant amount of hydrogen peroxide, compatible with the dramatic impairment of complex I activity [13]. We did not find a significant increase in hydrogen peroxide production during incubation of XTC.UC1 cells in DMEM-galactose using the same technique (results not shown). To reveal the occurrence of a shift of the cellular oxidation-reduction potential, we decided to assess glutathione homeostasis. Determination of reduced GSH and of its oxidation product GSSG, revealed a significant increase in the GSSG/GSH+GSSG ratio after 24 h of metabolic stress (Fig. 2E). This increase was mainly due to decreased levels of GSH (from 50.1±2.9 to 39.1±3.2 nmol/mg protein, n=3, in glucose and galactose respectively, $p<0.02$). These results reveal the occurrence of an oxidative imbalance in XTC.UC1 cells when forced to use impaired oxidative phosphorylation for energy production.

Bcl-2 overexpression inhibits actin cleavage. From previous studies it is known that the cytoskeleton can be stabilized by the anti-apoptotic Bcl-2 protein [10]. Furthermore, although Bcl-2 has no intrinsic antioxidant enzymatic or scavenging activity, it has been reported to display an antioxidant-like function by increasing the endogenous levels of GSH and inhibiting cell death elicited by the tripeptide depletion [6, 20]. Given that the endogenous Bcl-2 level of XTC.UC1 cells is lower than that of other cell lines derived from thyroid tumors, XTC.UC1 cells were transfected to overexpress Bcl-2. Positive clones were

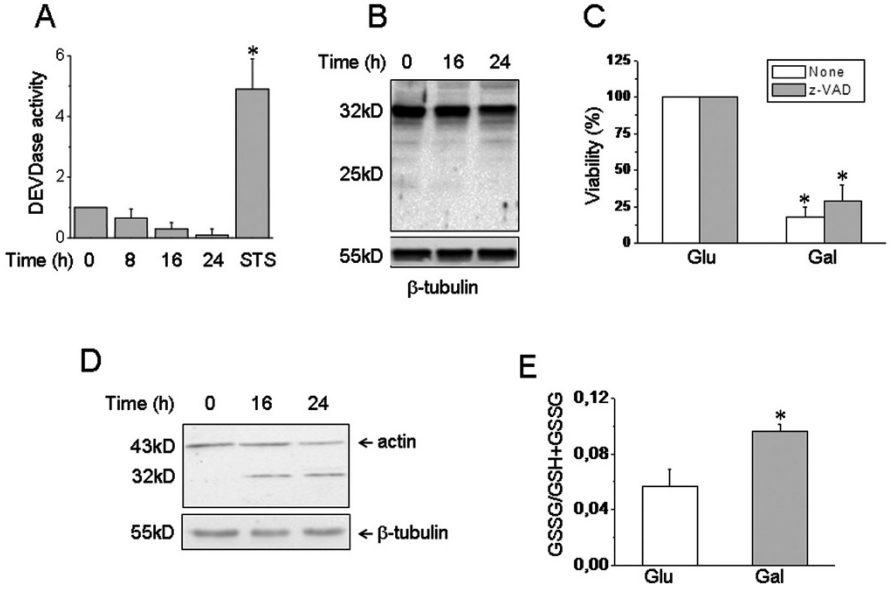

Figure 2. Caspase-3 activation, actin cleavage and glutathione homeostasis in XTC.UC1 cells incubated in DMEM (Glu) or DMEM-galactose (Gal). (*A*) Cells were incubated in DMEM (t=0), DMEM-galactose medium for the times indicated, or for 16 h in DMEM containing 1 μM staurosporine (STS). The DEVDase activity, determined in cell lysates from the fluorescence of the substrate 7-amino-4-methylcoumarin, N-acetyl-L-aspartyl-L-glutamyl-L-valyl-L-aspartic acid amide (Ac-DEVD-AMC), was expressed as a ratio of the fluorescence developed in DMEM (t=0). Data are means ± SD of at least three determinations. * Value significantly different from DMEM ($p<0.05$). (*B*) Cells were incubated in DMEM (t=0) or for the times indicated in DMEM-galactose and the levels of procaspase-3 (32 kDa) in cell lysates were determined by Western blotting, as described in the Materials and methods. β-Tubulin was used as a control for protein loading. One representative blot out of three similar blots is shown. (*C*) Cells were incubated in DMEM (Glu) or in DMEM-galactose (Gal) for 24 h in the absence or presence of 5 μM benzyloxycarbonyl-Val-Ala-Asp-fluoromethyl-ketone (z-VAD-fmk). Cell viability was assessed using the sulforhodamine B assay as described in Materials and methods. Data are means ± SD of three experiments. * Value significantly different from untreated cells (none, $p<0.05$). (*D*) Cells were incubated as in (*B*) and levels of actin in cell lysates were determined by Western blotting. β-Tubulin was used as a control for protein loading. One representative blot out of seven similar blots is shown. (*E*) Cells were incubated in DMEM (Glu) or DMEM-galactose (Gal) for 24 h and GSH and GSSG were determined as described in the Materials and methods. Data, expressed as GSSG/GSH+GSSG ratio, are means ± SD of at least three experiments. * Value significantly different from DMEM ($p<0.05$).

selected, in which Bcl-2 protein levels were significantly increased compared to mock-transfected cells (Fig. 3A). Noticeably, the GSH level of Bcl-2 cells was significantly higher than mock-transfected cells in DMEM and further increased in DMEM-galactose. By contrast, under the latter condition the GSH level of mock cells was markedly decreased (Fig. 3B). Accordingly, the GSSG/GSH+GSSG ratio did not change in Bcl-2 cells, whereas it increased significantly in mock cells incubated in galactose medium (Fig. 3C). Furthermore, inspection under the microscope clearly showed that Bcl-2 overexpression preserved cellular morphology (Fig. 3D) and markedly reduced cell detachment from the culture dish (Fig. 3E). Conversely, ATP levels of Bcl-2 cells determined after 24 h of metabolic stress were even lower than those of mock-transfected cells, suggesting that Bcl-2 had no beneficial effect on mitochondrial energetic function (Fig. 3F).

It is noteworthy that Bcl-2 overexpression completely inhibited actin cleavage induced by metabolic stress (Fig. 4A). To explore the hypothesis that Bcl-2 could influence cytoskeletal stability through a physical interaction with actin and/or tubulin, immunoprecipitation experiments were carried out. Figure 4B shows that both actin and tubulin interacted with Bcl-2. Similar results were obtained when cellular lysates were immunoprecipitated with anti-Bcl-2 and revealed with anti-actin and anti-tubulin (not shown). These results clearly indicate that Bcl-2 physically interacted with both proteins, suggesting that its effect on cell morphology/adhesion might result from a direct action on cytoskeletal components.

Exogenous GSH prevents actin cleavage. Given the effect of Bcl-2 overexpression on the GSH endogenous levels, we decided to test whether exogenous GSH could also improve cytoskeletal stability and ameliorate cell morphology and viability after metabolic stress. XTC.UC1 cells were incubated in DMEM-galactose with and without pre-treatment with 10 mM GSH, a concentration similar to that present in the cytosol [21]. Figure 5A shows that cell morphology in DMEM-galactose was markedly pre-

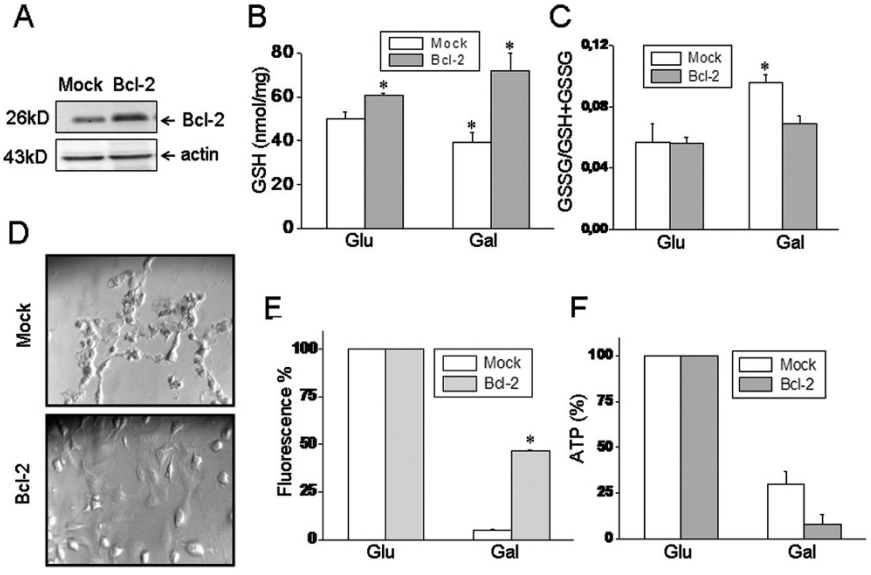

Figure 3. Effect of Bcl-2 on glutathione homeostasis, cellular morphology and ATP content. (*A*) Western blot of Bcl-2 levels in total cell lysates from XTC.UC1 cells transfected with empty-vector (mock) or with Bcl-2 (Bcl-2). Actin was used as a control for protein loading. One representative blot out of three blots is shown. (*B*) GSH levels were measured in mock and Bcl-2 cells in DMEM (Glu) or after 24-h incubation in DMEM-galactose (Gal). Data are means ± SD of three determinations. * Values significantly different from mock cells in DMEM ($p<0.05$). (*C*) Cells were treated as in (*B*) and the GSSG/GSH+GSSG ratio was determined as described in the Materials and methods. Data are means ± SD of at least three experiments. * Value significantly different from mock cells in DMEM ($p<0.05$). (*D*) Cellular morphology observed by optical phase-contrast microscopy of mock and Bcl-2 cells incubated for 24 h in DMEM-galactose. (*E*) Quantification of the percentage of adherent cells after 24-h incubation in DMEM (Glu) or in DMEM-galactose (Gal) by loading with 1 μM calcein-AM. Data are means ± SD of three determinations. * Value significantly different from mock cells in DMEM-galactose ($p<0.05$). (*F*) Mock and Bcl-2 cells were incubated for 24 h in DMEM-galactose (Gal) and the ATP content was determined as described in the Materials and methods. Data are expressed as percent of ATP levels determined in DMEM medium (Glu). Values are the mean ± SD of at least three experiments.

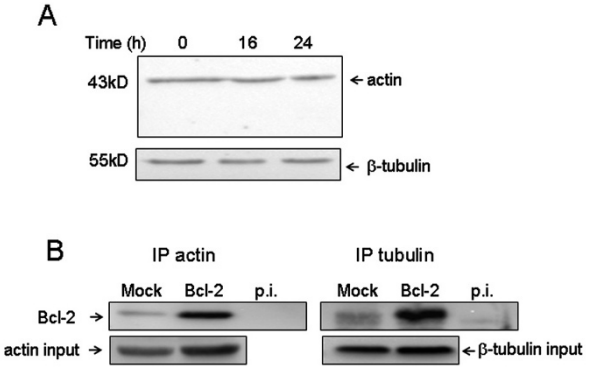

Figure 4. Actin levels and interaction with Bcl-2. (*A*) Actin levels in total cell lysates obtained from Bcl-2 cells during incubation in DMEM-galactose were determined by Western blotting, as described in Figure 2D. β-Tubulin was used as a control for protein loading. (*B*) Lysates from mock and Bcl-2 cells were immunoprecipitated with anti-actin, anti-β−tubulin, or with pre-immune serum (p.i.) and revealed with anti-Bcl2 as described in the Materials and methods. The reaction mixture prior to immunoprecipitation was analyzed by immunoblotting using anti-actin and anti-β-tubulin antibodies (input).

served in the presence of GSH, as also quantified by the significantly increased amount of adherent cells (Fig. 5B). Accordingly, actin cleavage triggered by metabolic stress was completely prevented by pre-incubation with exogenous GSH (Fig. 5C). Cell viability, however, was not improved (Fig. 5D).

Discussion

In this study we demonstrate that XTC.UC1 cells bearing a severe dysfunction in respiratory complex I, when forced to utilize solely oxidative phosphorylation for energy production, triggered a caspase-independent cell death pathway characterized by an imbalance of GSH homeostasis and a cleavage of the actin cytoskeleton. Both these events were completely inhibited by Bcl-2 overexpression. Prevention of actin breakdown by exogenous GSH indicates that Bcl-2 increases the cytoskeletal stability of XTC.UC1 cells mainly through an antioxidant function.

The present investigation into the molecular pathway of XTC.UC1 cell death triggered by metabolic stress showed that caspases were not involved. This conclusion is also supported by the lack of effect of the pan-caspase inhibitor z-VAD.fmk and by the finding that cytochrome c was not released into the cytosol following the death stimulus. Other mitochondrial

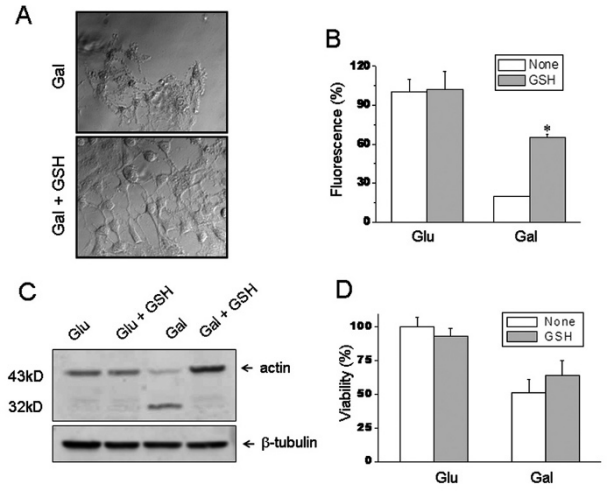

Figure 5. Effect of exogenous GSH on XTC.UC1 cells. (*A*) Cells were incubated for 24 h in DMEM-galactose (Gal) in the absence or presence of 10 mM GSH. Cellular morphology was observed by optical phase-contrast microscopy. Representative images out of five similar images are shown. (*B*) Quantification of the percentage of adherent cells was determined by loading with 1 μM calcein-AM. Data are means ± SD of three determinations. * Value significantly different from DMEM-galactose ($p<0.05$). (*C*) Cells were incubated in DMEM (Glu) or DMEM-galactose (Gal) in the absence or presence of 10 mM GSH. Actin levels in cell lysates were determined by Western blotting. β-Tubulin was used as a control for protein loading. One representative blot out of three similar blots is shown. (*D*) Cell viability was determined using the sulforhodamine B assay as described in the Materials and methods. Data are means ± SD of at least three experiments.

apoptogenic factors such as AIF and HtrA2/Omi, which are known to mediate caspase-independent death pathways [22, 23], were not implicated either. Furthermore, the integrity of the outer mitochondrial membrane suggests that the classical intrinsic pathway was not activated in this cell death process. This conclusion is also sustained by the lack of typical chromatin fragmentation, possibly due to a marked ATP depletion occurring during the metabolic stress condition [13]. In fact, an *in vitro* analysis of the nuclear changes arising during apoptosis has shown that ATP hydrolysis was required for completion of chromatin disassembly/fragmentation [24]. In spite of this, the mitochondria are likely to be responsible for the significant glutathione imbalance during glycolysis inhibition, when XTC.UC1 cells are forced to use the oxidative metabolism. The defective electron transport through the respiratory complex I hence leads to a shift of cellular oxidation-reduction potential, likely due to ROS overproduction.

We have previously reported that cells bearing missense mitochondrial DNA (mtDNA) mutations on ND subunits of complex I causing Leber's hereditary optic neuropathy (LHON) died through a caspase-independent death pathway when incubated in DMEM-galactose [25]. In these cells, however, cytochrome c, AIF and endonuclease G were released from the mitochondria, leading to nuclear chromatin fragmentation [15]. It is worth noting that the loss of viability of LHON cells during incubation in DMEM-galactose was not associated with alterations in cytoskeletal proteins (unpublished result). Furthermore, the GSH content of LHON cells was reported to be unchanged or even increased after metabolic stress [26]. It seems therefore that actin cleavage triggered by inhibition of the glycolytic pathway is associated with the presence of disruptive mtDNA mutations resulting in the decrease or loss of several complex I subunits [13] and glutathione imbalance. In this regard, a recent proteomic analysis revealed changes in the expression of cytoskeleton and cytoskeleton-associated proteins in cells lacking mtDNA or in the presence of respiratory chain inhibitors, suggesting a link between a severe energetic deficiency and cytoskeletal changes [3].

The question is then raised as to which protease is responsible for the observed actin cleavage. To identify this protease, inhibitors of serine proteases, lysosomal cathepsins D, E and B and calpains I and II were tested, but actin cleavage was not prevented (results not shown). It would therefore appear that some other, perhaps as of yet unknown protease, may be involved in the cleavage of actin observed during death of XTC.UC1 cells in DMEM-galactose.

We have shown here that Bcl-2 overexpression significantly preserved cell morphology, improved adhesion and inhibited actin cleavage, but was unable to ameliorate the viability of metabolically stressed XTC.UC1 cells. It has been previously proposed that Bcl-2 overexpression might have a protective function on mitochondrial physiology in cells bearing pathogenic mutations in mtDNA affecting the tRNA genes by regulating the levels of adenine nucleotides [27]. This does not occur in XTC.UC1 cells, possibly because the very severe energetic impairment caused by the MT-ND1 mutation in complex I, suggesting that not all mitochondrial dysfunctions can be rescued by Bcl-2 overexpression. Nevertheless, this anti-apoptotic protein affords protection against cytoskeletal damage of XTC.UC1 cells, in agreement with the stabilizing effect of Bcl-2 on the cytoskeleton previously described [10]. Bcl-2 contains four conserved domains denoted BH1–4. In particular, Bcl-2 has been shown to interact with tubulin through the BH3 domain [11] and with paxillin through the BH4 domain [12]. The immunoprecipitation experiments reported in the present study indicate that, in XTC.UC1 cells, Bcl-2 also interacts with actin. To the best of our knowledge this finding is novel and deserves further investigation to assess whether the two proteins directly interact or if other proteins are

required. Given that we have shown here that in XTC.UC1 cells actin interacts with Bcl-2 and that the latter affords protection against cytoskeletal actin breakdown, it is possible that binding of Bcl-2 to actin may mask critical amino acid residues and hinder its degradation at the site of cytoskeleton.

The other important finding of this study is that Bcl-2 overexpression significantly increases the amount of endogenous GSH and efficiently restores the glutathione homeostasis disturbed by metabolic stress. These data are in agreement with previous studies showing that Bcl-2 raised cellular antioxidant defense status, by increasing GSH levels [28] and Cu/Zn-superoxide dismutase (SOD1) activity [29]. Furthermore, a recent study has reported that Bcl-2 displays an antioxidant-like action at the site of mitochondria, due to a physical interaction between Bcl-2 and GSH, which could be disrupted by BH3 mimetics and BH3-only proteins [6]. Pre-treatment of XTC.UC1 cells with exogenous GSH increased cell adhesion and prevented actin cleavage, without influencing cell viability, exactly as observed in Bcl-2-overexpressing cells. Exogenous GSH did not further increase cell adhesion in Bcl-2-overexpressing cells (data not shown), also supporting the hypothesis for an antioxidant function of Bcl-2. In agreement with this, Bcl-2-overexpressing cells preserved cell adhesion, but failed to increase cell viability, even after an exogenous oxidative stress, *i.e.*, treatment with tert-butyl hydroperoxide (results not shown). We propose that re-establishment of glutathione homeostasis by either exogenous GSH or Bcl-2 overexpression can efficiently counteract oxidative stress caused by the forced use of the defective complex I, acting at the level of mitochondria [6]. This would hamper the signaling pathway involved in the activation of unknown protease(s), leading to actin cleavage. Although we show here that Bcl-2 physically interacts with actin, we cannot rule out the possibility that Bcl-2, bringing GSH to the cytoskeleton, might also act locally to preserve its integrity, through an independent mechanism. In this regard, actin has previously been shown to be a redox-sensitive protein [30]. Furthermore, actin has been suggested to be the most sensitive cytoskeleton component to oxidative stress, as one of its sulfhydryl groups is covalently modified by glutathionylation [31]. The decrease of GSH levels measured in XTC.UC1 cells after metabolic stress was not associated with a parallel increase of GSSG levels. This might be explained by the formation of mixed disulfides with actin sulfhydryl groups, although GSSG extrusion into the extracellular medium cannot be ruled out [32]. In conclusion, we demonstrate that Bcl-2 overexpression and exogenous GSH significantly increases cytoskeletal actin stability, suggesting that Bcl-2 can safeguard cellular morphology and adhesion through its antioxidant function.

Acknowledgements. This work was supported by grants from AIRC and PRIN-2006 (M.R.). We are indebted to Dr. Giovanni Manfredi, Weill Medical College of Cornell University, New York, USA, for the generous gift of the Bcl-2 plasmid. HtrA2/Omi antibody was kindly provided by Dr. Peter Vandenabeele, Department for Molecular Biomedical Research, Ghent University, Belgium.

1 Gourlay, C. W. and Ayscough, K. R. (2005) The actin cytoskeleton: A key regulator of apoptosis and ageing? Nat. Rev. Mol. Cell. Biol. 6, 583–589.
2 Rusanen, H., Annunen, J., Yla-Outinen, H., Laurila, A., Peltonen, J., Hassinen, I. E. and Majamaa, K. (2002) Cytoskeletal structure of myoblasts with the mitochondrial DNA 3243A>G mutation and of osteosarcoma cells with respiratory chain deficiency. Cell Motil. Cytoskeleton 53, 231–238.
3 Annunen-Rasila, J., Ohlmeier, S., Tuokko, H., Veijola, J. and Majamaa, K. (2007) Proteome and cytoskeleton responses in osteosarcoma cells with reduced OXPHOS activity. Proteomics 7, 2189–2200.
4 Li, P., Nijhawan, D., Budihardjo, I., Srinivasula, S. M., Ahmad, M., Alnemri, E. S. and Wang, X. (1997) Cytochrome c and dATP dependent formation of Apaf-1/caspase-9 complex initiates an apoptotic protease cascade. Cell 91, 479–489.
5 Orrenius, S., Gogvadze, V. and Zhivotovsky, B. (2007) Mitochondrial oxidative stress: Implications for cell death. Annu. Rev. Pharmacol. Toxicol. 47, 143–183.
6 Zimmermann, K. A., Loucks, F. A., Schroeder, E. K., Bouchard, R. J., Tyler, K. L. and Linseman, D. A. (2007) Glutathione binding to the Bcl-2 homology-3 domain groove: A molecular basis for Bcl-2 antioxidant function at mitochondria. J. Biol. Chem. 282, 29296–29304.
7 Susin, S. A., Zimzami, N. and Kroemer, G. (1998) Mitochondria as regulators of apoptosis: Doubt no more. Biochim. Biophys. Acta 1366, 151–165.
8 Vander Heiden, M. G., Chandel, N. S., Schumacker, P. T. and Thompson, C. B. (1999) Bcl-xL prevents cell death following growth factor withdrawal by facilitating mitochondrial ATP/ADP exchange. Mol. Cell 3, 159–167.
9 Vander Heiden, M. G., Chandel, N. S., Li, X. X., Schumacker, P. T., Colombini, M. and Thompson, C. B. (2000) Outer mitochondrial membrane permeability can regulate coupled respiration and cell survival. Proc. Natl. Acad. Sci. USA 97, 4666–4671.
10 Haldar, S., Basu, A. and Croce, C. M. (1997) Bcl-2 is the guardian of microtubule integrity. Cancer Res. 57, 229–233.
11 Knipling, L. and Wolff, J. (2007) Direct interaction of Bcl-2 proteins with tubulin. Biochem. Biophys. Res. Commun. 341, 433–439.
12 Sorensen, C. M. (2004) Interaction of Bcl-2 with paxillin through its BH4 domain is important during ureteric bud branching. J. Biol. Chem. 279, 11368–11374.
13 Bonora, E., Porcelli, A. M., Gasparre, G., Biondi, A., Ghelli, A., Carelli, V., Baracca, A., Tallini, G., Martinuzzi, A., Lenaz, G., Rugolo, M. and Romeo, G. (2006) Defective oxidative phosphorylation in thyroid oncocytic carcinoma is associated with pathogenic mitochondrial DNA mutations affecting complexes I and III. Cancer Res. 66, 6087–6095.
14 Zielke, A., Tezelman, S., Jossart, G. H, Wong, M., Siperstein, A. E., Duh, Q. Y. and Clark, O. H. (1998) Establishment of a highly differentiated thyroid cancer cell line of Hürthle cell origin. Thyroid 8, 475–483.
15 Zanna, C., Ghelli, A., Porcelli, A. M, Carelli, V., Martinuzzi, A. and Rugolo, M. (2005) Caspase-independent death of Leber's hereditary optic neuropathy cybrids is driven by energetic

failure and mediated by AIF and endonuclease G. Apoptosis 10, 997–1007.
16 Bradford, M. M. (1976) A rapid and sensitive method for the quantitation of microgram quantities of protein utilizing the principle of protein-dye binding. Anal. Biochem. 72, 248–254.
17 Ghelli, A., Porcelli, A. M., Zanna, C., Martinuzzi, A., Carelli, V. and Rugolo, M. (2008) Protection against oxidant-induced apoptosis by exogenous glutathione in Leber hereditary optic neuropathy cybrids. Invest. Ophthalmol. Vis. Sci. 49, 671–676.
18 Scarlatti, F., Sala, G, Somenzi, G., Signorelli, P., Sacchi, N. and Ghidoni, R. (2003) Resveratrol induces growth inhibition and apoptosis in metastatic breast cancer cells *via de novo* ceramide signalling. FASEB J. 17, 2339–2341.
19 Robinson, B. H., Petrova-Benedict, R., Buncic, J. R. and Wallace, D. C. (1992) Nonviability of cells with oxidative defects in galactose medium: A screening test for affected patient fibroblasts. Biochem. Med. Metab. Biol. 48, 122–126.
20 Kane, D. J., Sarafian, T. A., Anton, R., Hahn, H., Gralla, E. B., Valentine, Ord, T. and Bredesen, D. E. (1993) Bcl-2 inhibition of neural death: Decreased generation of reactive oxygen species. Science 262, 1274–1277.
21 Hwang, C., Sinskey, A. J. and Lodish, H. F. (1992) Oxidized redox state of glutathione in the endoplasmic reticulum. Science 257, 1496–1502.
22 Modjtahedi, N., Giordanetto, F., Madeo, F. and Kroemer, G. (2006) Apoptosis-inducing factor: Vital and lethal. Trends Cell Biol. 16, 264–272.
23 Suzuki, Y., Imai,Y., Nakayama, H., Takahashi, K., Takio, K. and Takahashi, R. (2001) A serine protease, HtrA2, is released from the mitochondria and interacts with XIAP, inducing cell death. Mol. Cell 8, 613–621.
24 Toné, S., Sugimoto, K., Tanda, K., Suda, T., Uehira, K., Kanouchi, H., Samejima, K., Minatogawa, Y. and Earnshaw W. C. (2007) Three distinct stages of apoptotic nuclear condensation revealed by time-lapse imaging, biochemical and electron microscopy analysis of cell-free apoptosis. Exp. Cell Res. 313, 3635–3644.
25 Ghelli, A., Zanna, C., Porcelli, A. M, Schapira, A. H., Martinuzzi, A., Carelli, V. and Rugolo, M. (2003) Leber's hereditary optic neuropathy (LHON) pathogenic mutations induce mitochondrial-dependent apoptotic death in transmitochondrial cells incubated with galactose medium. J. Biol. Chem. 278, 4145–4150.
26 Floreani, M., Napoli, E., Martinuzzi, A., Pantano, G., De Riva, V., Trevisan, R., Bisetto, E., Valente, L., Carelli, V. and Dabbeni-Sala, F. (2005) Antioxidant defences in cybrids harboring mtDNA mutations associated with Leber's hereditary optic neuropathy. FEBS J. 272, 1124–1135.
27 Manfredi, G., Kwong, J. Q., Oca-Cossio, J. A., Woischnik, M., Gajewski, C. D., Martushova, K., D'Aurelio, M., Friedlich, A. L. and Moraes, C. T. (2003) Bcl-2 improves oxidative phosphorylation and modulates adenine nucleotide translocation in mitochondria of cells harboring mutant mtDNA. J. Biol. Chem. 278, 5639–5645.
28 Ellerby, L. M., Ellerby, H. M., Park, S. M., Holleran, A. L., Murphy, A. N., Fiskum, G., Kane, D. J., Testa, M. P., Kayalar, C. and Bredesen, D. E. (1996) Shift of the cellular oxidation-reduction potential in neural cells expressing Bcl-2. J. Neurochem. 67, 1259–1267.
29 Lee, M., Hyun, D. H., Marshall, K. A., Ellerby, L. M., Bredesen, D. E., Jenner, P. and Halliwell, B. (2001) Effect of overexpression of Bcl-2 on cellular oxidative damage, nitric oxide production, antioxidant defenses, and the proteasome. Free Radic. Biol. Med. 31,1550–1559.
30 Laragione, T., Bonetto, V., Casoni, F., Massignan, T., Bianchi, G, Gianazza, E. and Ghezzi, P. (2003) Redox regulation of surface protein thiols: Identification of integrin alpha-4 as a molecular target by using redox proteomics. Proc. Natl. Acad. Sci. USA 100, 14737–14741.
31 Dalle-Donne, I., Rossi, R., Milzani, A., Di Simplicio, P. and Colombo, R. (2001) The actin cytoskeleton response to oxidants: From small heat shock protein phosphorylation to changes in the redox state of actin itself. Free Radic. Biol. Med. 31, 1624–1632.
32 Filomeni, G., Rotilio, G. and Ciriolo, M. R. (2002) Cell signalling and the glutathione redox system. Biochem. Pharmacol. 64, 1057–1064.